ELSEVIER

Biophysical Chemistry 57 (1996) 261–267

Biophysical Chemistry

Monte Carlo studies on potentiometric titration of (carboxymethyl)cellulose

Takuhiro Nishio *

Department of Physics, Hamamatsu University School of Medicine, Hamamatsu 431-31, Japan

Received 19 January 1995; revised 23 February 1995; accepted 13 March 1995

Abstract

Monte Carlo simulations of the potentiometric titration are carried out for (carboxymethyl)cellulose in aqueous salt solutions by a previously developed method. A nearly elliptic cylinder with spherical ionizable groups is assumed as model of (carboxymethyl)cellulose molecule. The spherical charges with a hard core potential are adopted as mobile hydrated ions. A fairly satisfactory agreement of the titration curves with the experimental data is achieved by using reasonable molecular dimensions. Dependence of the calculated titration profiles on the molecular model and the characteristics of the system are discussed.

Keywords: Potentiometric titration; (Carboxymethyl)cellulose (CMC); Monte Carlo simulation; Linear polyelectrolyte; Cylindrical cell system

1. Introduction

Potentiometric titration is an important index of the polyelectrolyte solutions because of its straight relation to the electrostatic free energy with the ionization of the polyion [1]. Several theories had been proposed to explain the titration curves of the linear polyelectrolytes [2–7]. These theories have been improved and applied to various polyelectrolytes in recent studies [8–11]. Each treatment was, however, found to be more or less insufficient because it included some defects due to its own approximating procedure.

The Monte Carlo (MC) method was developed for the potentiometric titration of cylindrical polyelectrolytes, and the electrostatic free energy was analyzed by the author in case of no added salt [12]. The deviation of the MC simulation from the solution of the Poisson–Boltzmann (PB) equation was revealed to be due to the difference of the electrostatic energy between both systems. Detailed analysis of the titration behavior was found to be possible by this simulation method.

(Carboxymethyl)cellulose (CMC) is one of the most investigated linear polyelectrolytes. The CMC molecule takes an extended form due to its stiff cellulose backbone even in the absence of charge [13]. Its potentiometric titration behavior was studied by several research groups [14–17]. Muroga et al. measured the considerably fine titration curves of the NaCl solution and fitted by the numerical solution of

* Corresponding author.

SSDI 0301-4622(95)00057-7

the PB equation [18]. Their fitting, however, was satisfactory only at high charge densities. Furthermore, the effect of the mobile ion size to the electrostatic potential was ignored in their calculations.

In the present study, an attempt is made on the MC simulations of the potentiometric titration of CMC in aqueous salt solution. A comparison is made between the results of the MC simulation and the data from Muroga et al. A fairly satisfactory agreement with the experimental data is achieved by adopting a simplified but reasonable molecular model.

2. Model and method

2.1. Algorithm of the MC simulation in cylindrical cell system

The details of the computational method were described in the previous paper [12]. Its essence and the improvements are noted here.

An aqueous CMC solution is treated as an isolated cylindrical cell system. A rigid rod of the modeled CMC molecule is centered in the objective cell. The number of the carboxyl group attached to the rod, N_P, is proportional to the height of the cell, equal to the length of the molecular model of CMC, H. The cell radius, R, is determined by the concentration of the carboxyl group in the solution, C_P. The cell dimensions are determined on account of the accuracy and the CPU time for the calculation. Two long external cells are attached to both sides of the objective cell to eliminate the end effect. The contribution of the energy from the external cells becomes too large and disturbs the equilibrium state when the excessively oblate objective cell is adopted. Then, the restriction of the cell dimensions, $R \leqslant 2.5\ H$, is always kept in the adjustment of the size of the objective cell.

The neutral un-ionized carboxyl group, with its own intrinsic dissociation constant K_0, can dissociate into a mobile counterion and an ionized group by the ionization. The N_S cations and the same number of anions from the 1:1 salt are distributed in the cell.

The MC trial in the iterative loop of the simulation consists of the following four processes:
(1) ionization of an un-ionized group;
(2) deionization of an ionized group;
(3) movement of a counterion;
(4) movement of an ion from added salt.
If the group is in the un-ionized state, process (1) is tried or nothing is done. If the group is ionized, (2) or (3) is chosen in the given probability. Trial process (4) is added to the simulation in case of the salt solution.

The energy change with the ionization is determined by the difference of the aqueous pH and $\mathrm{p}K_0$. The $\mathrm{p}K_0$ is the negative logarithm of K_0. The intrinsic $\mathrm{p}K_0$ value of carboxyl group is defined in the infinitely dilute solution without added salt.

The movement of mobile ions is attempted in the Cartesian coordinates with the regulated step width. In the previous simulation, if the new axial position, z, was less than zero or greater than H, the z component was replaced into the objective cell, and x and y were multiplied by -1. This replacement of the x and y component for mixing seems to be unnecessary. Then, the z component is only replaced in the present computation.

The average degree of ionization, α, and other averaged values are obtained in an iterative loop after the convergence is fulfilled. The negative logarithm of the apparent dissociation constant, $\mathrm{p}K_\mathrm{a}$ and the electrostatic term of $\mathrm{p}K_\mathrm{a}$, $\Delta\mathrm{p}K$, is related to a given solution pH, $\mathrm{p}K_0$, and α, expressed by the following equation:

$$\Delta\mathrm{p}K = \mathrm{p}K_\mathrm{a} - \mathrm{p}K_0 = \mathrm{pH} - \mathrm{p}K_0 + \log[(1-\alpha)/\alpha]. \quad (1)$$

The $\Delta\mathrm{p}K$ is evaluated using a given $\mathrm{pH} - \mathrm{p}K_0$ value and an averaged degree of ionization, α. The $\mathrm{p}K_\mathrm{a}$ value is determined by adding a suitable $\mathrm{p}K_0$ value to the $\Delta\mathrm{p}K$. Then, the titration curve can be compared with the experimental data.

2.2. Molecular model

The present work is planned to compare the MC results with the titration data of the CMC in the aqueous NaCl solution by Muroga et al. [18]. The CMC molecule was treated as one of the worm-like chain polyelectrolytes in the recent work [19]. In the present simulation, however, the molecule is treated as the rigid structure based on the molecular model

from the x-ray fiber diffraction of cellulose [20]. The ribbon-like cellulose backbone is treated as a nearly elliptic cylinder, and the carboxylic acid group attached to the backbone is assumed as a sphere. The counterion from the ionized group as well as the ion from the salt, NaCl, is also treated as a sphere. The CMC molecule and all mobile ions are assumed to interact with a hard core potential and an electrostatic potential. The energy between two charged species, labeled as i and j, is defined as the Coulombic interaction with the hard core repulsion, as follows ($\phi_{i,j}$ was used in Eq. (9) of Ref. [12] instead of $u_{i,j}$):

$$u_{i,j} = \begin{cases} \dfrac{1}{4\pi\epsilon_0 D}\dfrac{q_i q_j}{|\boldsymbol{r}_i - \boldsymbol{r}_j|} & |\boldsymbol{r}_i - \boldsymbol{r}_j| > \sigma_i + \sigma_j \\ \infty & |\boldsymbol{r}_i - \boldsymbol{r}_j| \leqslant \sigma_i + \sigma_j \end{cases} \quad (2)$$

where q, $\boldsymbol{r}$ and σ with subscript i or j denote the charge, the position and the radius of the each species, respectively, ϵ_0, the permittivity of the vacuum, and D, the relative dielectric constant of the solvent. The numerical constants used in the simulation are $D = 78.55$ and the absolute temperature $T = 298.15$ K. The details of the practical calculation are the same as in the previous paper [12].

The model of the CMC molecule adopted in this study is represented in Fig. 1. The impenetrable backbone of CMC is for simplicity assumed to be a nearly elliptic cylinder. The elliptic cross section of the volume from which the mobile ions are excluded is expressed as:

$$\frac{x^2}{(a_x + \sigma_m)^2} + \frac{y^2}{(a_y + \sigma_m)^2} = 1 \quad (3)$$

where a_x and a_y are the x and y components of the radius of the backbone rod; σ_m is the radius of the mobile ion. The value of a_x and a_y in the nearly elliptic model are 4 Å and 1.5 Å, respectively. The truly cylindrical model ($a_x = a_y = 4$ Å) is also tested to examine the effect of the rod shape. The carboxyl groups are assumed to be located on x axis to simplify the model. The distance of the center of each group from the origin of the axis, r_P, is estimated at 6 Å (Fig. 1a).

The degree of carboxymethyl substitution (DS) of CMC measured by Muroga et al. was 1.54 [18].

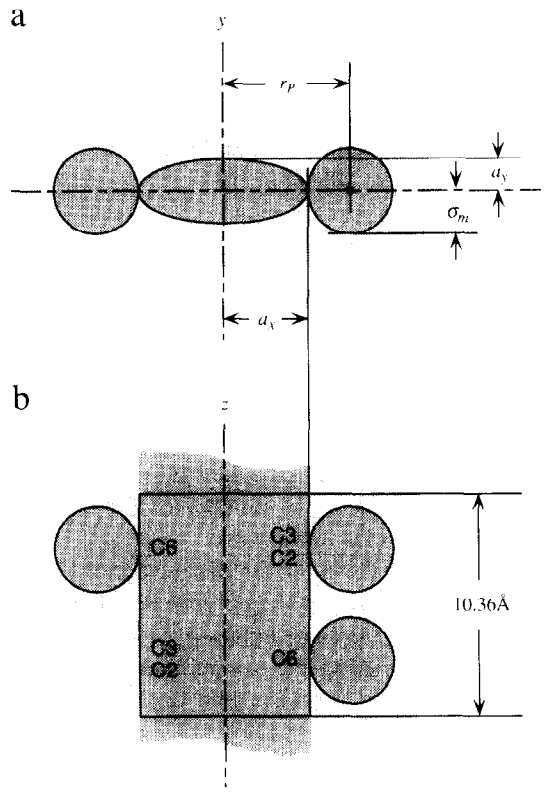

Fig. 1. Model of the molecular rod of the CMC cellobiose unit. The cellulose backbone is modeled as a nearly elliptic cylinder. The carboxyl group is assumed as a sphere. Dark area is the hard core of molecular model and light area represents the volume from which the centers of the mobile ions are excluded. (a) top view, (b) side view. See text for parameters.

Then, the number of the carboxylic acid attached to the glucose monomer is decided to be a close value to 1.5 (three substitutions per cellobiose unit) in the present simulations. The length of the cellobiose unit (two monomers) is defined to be 10.36 Å, equal to that of cellulose II [20]. The mean axial distance of the group, b, and the linear charge density parameter at fully ionized state, $\xi^{\max}$, are 3.453 Å and 2.066, respectively.

The location of carboxyl groups on the cylinder is assumed as follows, although their precise locations on the cellulose backbone are unknown.

The carboxyl groups are attached at every C6 position of the glucose monomer and attached at the C2 or C3 position in the probability 0.5, because the C6 position is believed to be preferentially substi-

tuted and the substitution of both the C2 and C3 position seems to be rare due to the steric hindrance. The location of the group at C2 and C3 cannot be distinguished. Then, it is assumed that the group at C2 or C3 have the same z component as the group at C6 on the opposite side (Fig. 1b).

Various group arrangements are possible within the above requirements. Two typical arrangements are examined in the present work, as shown in Fig. 2. The groups are attached at every C6 position in both arrangements. In arrangement I, the groups attached alternatingly at C2 or C3 positions. The two third of the groups attached to one side of the rod. On the other hand, two groups attached continually at C2 or C3, and two non-attached sites are spaced in arrangement II. The same number of groups is arranged on both sides in this case.

The result of the simulation depends on the radius of the ionizable group on the polymer rod and that of the mobile ions. The same value, σ_m, is adopted as a radius of all charged species to facilitate the analysis. This simplification is reasonable according to the estimation of the effective hydrated radius of the groups for the other properties [21]. Though the radius of the ionizable group must be different between the ionized and un-ionized states due to the hydration, it is fixed as σ_m to simplify the calculation. The radius of the ions adopted in the previous MC simulations is in the range from 2 to 3 Å. In this study, the smallest value in the range, 2 Å, is adequate to fit the experimental data.

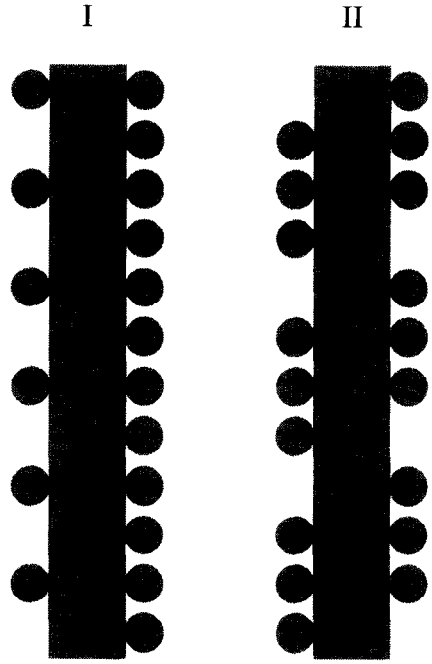

Fig. 2. Schematic views of two examined arrangements (I and II) of the carboxyl groups on the CMC backbone rod (see text).

3. Results and discussion

3.1. Dependence of titration on the molecular model

At first, the dependence of the titration curve on the rod shape is examined when the distance of the center of each group from the axis origin, r_P, is not changed (6 Å). The case of an elliptic cylinder ($a_x = 4$ Å, $a_y = 1.5$ Å) and of a cylindrical rod ($a_x = a_y = 4$ Å) are represented at $C_S = 0.01$ M with the experimental data in Fig. 3a. The group arrangement I is adopted and the given pK_0 value is 3.62 in both cases. A small but distinguishable deviation appears in the range of $\alpha > 0.5$ in the case of a cylindrical rod. The data fitting becomes poorer by the increase of the radius of the backbone rod in high α ranges. Similar divergence occurs by increasing the radius of the ionizable group and/or the radius of the mobile ions. This means that the change of the volume from which the mobile ions are excluded is effective to the electrostatic free energy with the ionization process. In the case of higher C_S, a similar tendency is observed. The counterion concentration is higher at the thin (nearly elliptic) model for the CMC backbone. The Manning's radius of the thin model is about 1 Å smaller than the case of the thick (truly cylindrical) model. The increase of the counterion in the proximity of the polyion charge decreases the electrostatic energy term contributed by the polyion–counterion interaction. Because the decrease due to this energy term is larger than the term due to the increase by the counterion accumulation, the total electrostatic energy (enthalpy) decreases in the thinner backbone model as a result.

The effect of the difference in the group arrangement is shown in Fig. 3b. The nearly elliptic model is used as the rod shape in both cases. The decrease of the pK_a in a high α range is observed in the

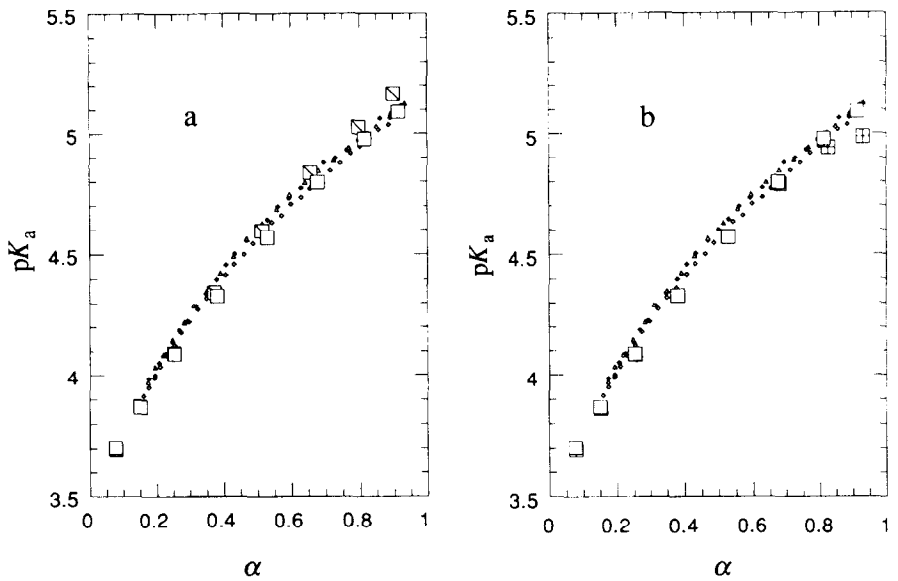

Fig. 3. The dependence of the titration curve on the CMC molecular model. The results of the MC simulations (large symbols) are represented with the experimental data (small symbols) obtained by Muroga et al. at $C_S = 0.01$ M [18]. Three small symbols represent the difference of the polymer concentration C_P (△ 0.0044, ◇: 0.0057, ◆: 0.0084 N). The given pK_0 value is 3.62 in all cases. (a) The effect of the rod shape; (□) the case of an elliptic cylinder ($a_x = 4$ Å, $a_y = 1.5$ Å) and (□, with \) that of a cylindrical rod ($a_x = a_y = 4$ Å). (b) The comparison of the group arrangements; (□) arrangement I and (⊞) arrangement II.

arrangement II. No remarkable difference of the ion distribution is observed between both molecular models even at $\alpha = 1$. This divergence of the titration curve is due to the slight difference of the electrostatic energy and the entropy of the mixing of the state of ionizable groups. Comparing the mixing entropy of the state, it is found that in arrangement II there are a higher number of acceptable cases in the ionization pattern where the electrostatic energy is smaller than that of arrangement I at a high α range. This seems to be due to the balanced allocation of the groups in arrangement II. This causes the decrease of the electrostatic free energy and the downward deviation of the titration curve. This observation suggests the asymmetry of the group arrangement on the rod of the CMC molecules. It cannot be concluded that the arrangement I is a unique one to fit the data, however. Other arrangements are also possible to match the simulations to the experimental data.

Table 1
Parameters of the objective cell for the MC simulation

Label	C_P (N)	C_S (M)	N_P	N_S	R (Å)	H (Å)	MCS	Symbol
A-a1	0.005	0.01	36	72	174.963	124.32	5000	□
B-a2	0.005	0.02	30	120	174.963	103.60	4000	□
B-b1	0.0075	0.02	36	96	142.857	124.32	5000	○
C-b3	0.0075	0.05	24	160	142.857	82.88	4000	○
C-c2	0.01	0.05	30	150	123.717	103.60	4000	◇
D-c4	0.01	0.1	18	180	123.717	62.16	4000	◇
D-d3	0.015	0.1	24	160	101.015	82.88	4000	△
E-d4	0.015	0.2	18	240	101.015	62.16	3000	△

MCS is the number of the Monte Carlo step per charged group for a titration point. Symbols in the most right row are used in Fig. 4. See text for other parameters.

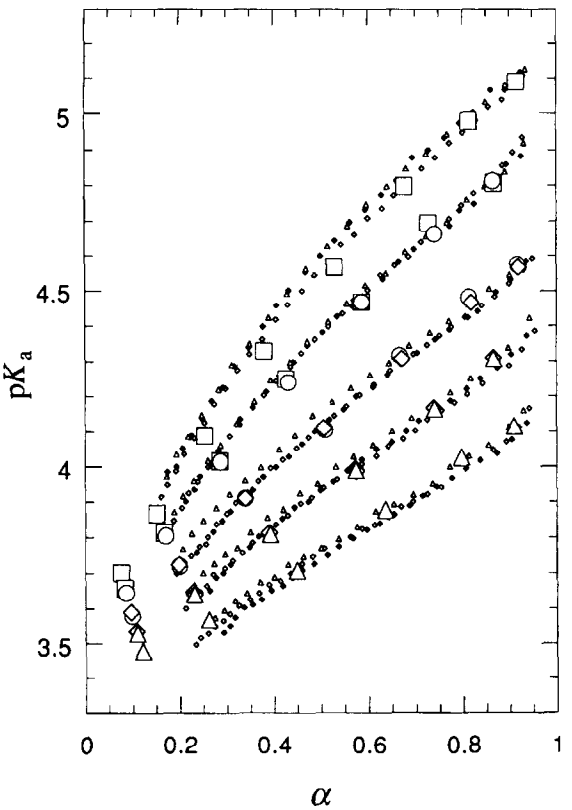

Fig. 4. The dependence on the salt concentration of the titration curve. The rod is an elliptic cylinder and the arrangement I is adopted. C_S = 0.01, 0.02, 0.05, 0.1, 0.2 M from top to bottom (see text and Table 1). For small symbols of the experimental data see Fig. 3.

3.2. Dependence on salt concentration

The dependence on the 1:1 salt (NaCl) concentration is investigated using the elliptic cylinder model and group arrangement I. The parameters of the calculation for each simulation are presented in Table 1. When the cell height must be compressed at high salt concentration, the cell radius is decreased to eliminate the excessively oblate cell shape. Then, the simulations at two polymer concentrations are attempted to check the dependence on the polymer concentration, C_P, in several cases of the same salt concentration. The given pK_0 value is 3.62 in all cases. The obtained titration curves are shown with the experimental data in Fig. 4.

The agreement of the MC results with the experimental data is satisfactory in each salt concentration and in a whole α range. The agreement becomes better in the higher salt concentration, since the upward shift in the range of $\alpha = 0.2$ to 0.4 of the experimental results is disappeared. It seems that the C_P dependence can be ignored in the condition of the simulation. The C_P dependence was not observed experimentally. It is noteworthy that the agreement is achieved using common pK_0 value at each salt concentration. The downward shift of pK_a due to the increase of the salt concentration is well reproduced without other hypotheses.

In the present simulation, the CMC molecule is treated as a simple rigid model. The ionic interaction is also reduced to the electrostatic interaction and the hard-core potential. It seems that the model used here is not a solitary case. Another combination is probably possible for the molecular model, its sizes, and its interactions. Various refinements applied to the DNA solution are not only possible but also necessary [22,23]. Furthermore, the effect of the chain flexibility cannot be ignored. The simplifications in the simulation, however, are quite reasonable and suitable to fit the experimental data. In a real solution system, several effects neglected here may cancel each other. For example, a similar fitting may be obtained by adopting the dielectric discontinuity around the CMC and the larger ion size. More information on the system is required for further refinement.

4. Conclusion

The potentiometric titration curves of CMC in NaCl solution are well reproduced by the present MC simulation. The molecular model and its interactions adopted here is extremely simplified. It is notable that this simple model is still efficient in the present stage. Another more precise model seems also possible to fit the experimental data in case that more information is obtained about CMC molecules. Further studies are required for the titration of other linear polyelectrolytes and the other colligative properties to recognize the efficiency and the restriction of this molecular model.

Acknowledgements

The author is grateful to Professor A. Minakata for valuable suggestions and critical reading of the manuscript and Mr. Y. Nozue for technical support.

References

[1] A. Katchalsky and J. Gillis, Rec. Trav. Chim., 68 (1949) 879.
[2] A. Katchalsky, J. Mazur and P. Spitnik, J. Polym. Sci., 23 (1957) 513.
[3] L. Kotin and M. Nagasawa, J. Chem. Phys., 36 (1962) 873.
[4] M. Nagasawa, Pure Appl. Chem., 26 (1971) 519.
[5] A. Minakata, K. Matsumura, S. Sasaki and H. Ohnuma, Macromolecules, 13 (1980) 1549.
[6] S. Sasaki and A. Minakata, Biophys. Chem., 11 (1980) 199.
[7] G.S. Manning, J. Phys. Chem., 85 (1981) 870.
[8] S. Kawaguchi, T. Kitano, K. Ito and A. Minakata, Macromolecules, 23 (1990) 731.
[9] T. Nishio, Biophys. Chem., 40 (1991) 19.
[10] C.P. Woodbury, Jr., J. Phys. Chem., 97 (1993) 3623.
[11] R.G. Smits, G.J.M. Koper and M. Mandel, J. Phys. Chem., 97 (1993) 5745.
[12] T. Nishio, Biophys. Chem., 49 (1994) 201.
[13] C. Tanford, Physical Chemistry of Macromolecules, John Wiley and Sons, New York, 1961.
[14] D.T.F. Pals and J.J. Hermans, Rec. Trav. Chim., 71 (1952) 513.
[15] N.S. Schneider and P. Doty, J. Phys. Chem., 58 (1954) 762.
[16] M. Mandel, J. Polym. Sci. Part A-2, 8 (1970) 1841.
[17] M. Rinaudo and M. Milas, Macromolecules, 6 (1973) 879.
[18] Y. Muroga, K. Suzuki, Y. Kawaguchi and M. Nagasawa, Biopolymers, 11 (1972) 137.
[19] R.M. Davis, Macromolecules, 24 (1991) 1149.
[20] J. Blackwell, K.H. Gardner, F.J. Kolpak, R. Minke and W.B. Claffey, in A.D. French and K.H. Gardner (Editors), Fiber Diffraction Methods, American Chemical Society, Washington, DC, 1980, p. 315.
[21] J. Kielland, J. Am. Chem. Soc., 59 (1937) 1675.
[22] B. Jayaram, S. Swaminathan, D.L. Beveridge, K. Sharp and B. Honig, Macromolecules, 23 (1990) 3156.
[23] B. Jayaram and D.L. Beveridge, J. Phys. Chem., 95 (1991) 2506.